Study of Parameter Influence on Quality on the Electromagnetic Imaging Reconstruction from the Spectrum of the Diffracted Field: Application to Reconstruction of the leakage Current of ISM Applicators

Y. Mejdoub[1], A. Ghammaz[2], H. Rouijaa[3], and K. Senhaji Rhazi[1]

[1]Laboratory of Networks, Computer Science, Telecommunication, Multimedia (RITM), Higher School of Technology ESTC, Hassan II University, Casablanca, Morocco
[2]Laboratory of Electrical Systems and Telecommunications, Faculty of Sciences and Technology, Cadi Ayyad university, Marrakech, Morocco
[3]Laboratory for Systems Analysis and Information Processing, Faculty of Sciences and Technology, Hassan I University, Settat, Morocco
*corresponding author, E-mail: ymejdoub@yahoo.fr

Abstract

The ISM applicators generate leakage currents that can disrupt satellite TV transmission, taking into account the effects of the electromagnetic waves and those of the CEM. We are interested in these as a way to reconstitute their leakage currents, using the Micro-waves Imagery. We propose such a method of spectral analysis, which is intended to reconstruct the equivalent current distribution (position and form) to an object starting from the diffracted field spectrum by the Micro-waves Imagery. Our contribution resides in the influence of different parameters (N number of the measurement point, and the distance z0 of the measurement plane) on the reconstitution quality. This method is presented and illustrated; an algorithm of reconstructing the image of an object existing within a surrounding homogenous medium with known dielectric properties is developed by MATLAB.
. This method leads to more significant results, and quickly permits to get information about the object form.

1. Introduction

The Microwave Tomography has received intense attention as an imaging modality. Therefore, extensive research has been conducted in this field during the last 40 years. This is due to the versatility and suitability of this imaging technique for a wide range of applications such as industrial non-destructive testing [1], medical imaging [2], and through-wall imaging [3,4]. The use of electromagnetic fields for the purpose of quantitatively determining the inner structure of objects leads to inverse mathematical problems.
Within the scope of the account of electromagnetic compatibility EMC, the electromagnetic perturbations produced by the industrial generators of high frequencies and microwaves can, in some cases, blur the reception of radio engineering, degrade the quality or even the function of other equipment situated either in their near environment or in that which is relatively remote. In this respect, the ISM applicators (Scientific and Medical Industrials) are a good example in that they generate leakage currents that can disrupt TV transmission through satellite [5,6,7].
The objective of a large number of methods has been to reconstitute objects using microwaves imagery. The first methods of reconstruction in microwave tomography date back to the 1980s and consisted of a qualitative estimation [8,9]. The basic aim of such methods has been to represent the object using induced unknown currents which are directly related to a diffracted field in a linear manner.
Most of these methods are applied to 2D problems. Among these is the technique of image reconstruction using projections of different views of the object [10], iterative numeric methods for the electromagnetic imaging based on Newton Kantorovitch's process or that of the conjugate Gradient, which allows to reconstruct the complex dielectric constant of the objects [11,12,13,14], and the method of spectral analysis that reconstructs the current distribution of an object from the spectrum of the diffracted field [15].
Such leakage currents can be modeled through distributing an equivalent current. The first objective of this article is to theoretically present an analytical method of reconstituting these currents, which are based on the spectral analysis of the field diffracted by the microwave imagery [15], and to implementing, under MATLAB, an algorithm that permits to determine the position and the form of the object existing within a homogenous milieu surrounding known dielectric properties. And the second objective is to study the influence of different parameters (N number of the measurement point, and the distance z0 of the measurement plane) on the reconstitution quality.
Methodologically, the first section of this paper will be devoted to explain the principle of the method of reconstruction. The next part will present the object reconstruction results from simulation data and study of the influence of different parameters on the reconstitution quality. Then we will draw some conclusions.

2. Diffracted electric field

We submitting an object (volume V), of an electromagnetic radiation, a diffracted field dependent on the characteristics of the object will be generated. The principle of micro-waves imagery, having the end of the inverse diffraction, is

able to reconstruct the most possibly accurate image of the object existing within a milieu.

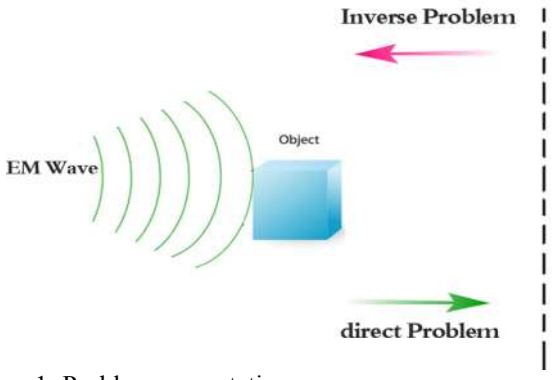

Figure 1: Problem presentation.

The direct problem in our study corresponds to calculation of the diffracted electric field Ed which is dispersed from a known distribution of permittivity ε, permeability μ and its conductivity σ in an investigation domain D when a known incident field Einc (Fig. 1). The direct problem can always be solved by using numerical methods such as the Moments method [12][16,17,18], the finite element method (FEM) in hybrid with the boundary elements (BE) [19,20] or in some cases the Finite Difference Methods (FDM) [4] [21].
The inverse problem is to recover the current distribution of an object, from the diffracted field measured around the object. In general a multi-view is necessary, in order to collect enough independent data. In addition, the measurement distance and the number of the received points have an impact on the object reconstruction

2.1. Diffracted electric field expression

We consider the propagation of electromagnetic waves in a homogeneous medium characterized by its electrical permittivity ε1, its magnetic permeability μ1 and its conductivity σ1. In this medium a volume V (object) exists, this volume V of substance is characterized by an electrical permittivity ε2, a magnetic permeability μ2 and its conductivity σ2.

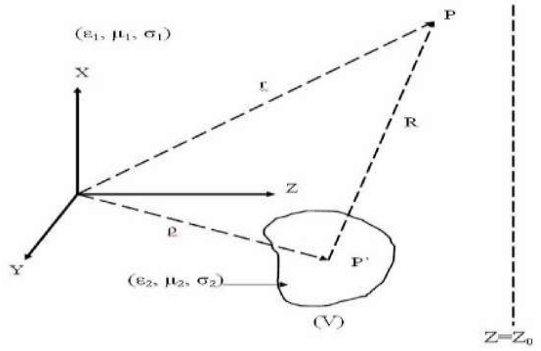

Figure 2: Vectors presentation

In the three-dimensional system of Cartesian coordinates, either $\vec{r}$ a position vector identifying a point P outside the volume (V), in the medium (ε1, μ1, σ1), and either $\vec{\sigma}$ the vector identifying a point P' Inside the volume (V), as shown in Fig. 2.

By definition [11], the diffracted electric field is the difference between the field $\vec{E}_2(\vec{r},t)$ measured in the presence of the volume and the field $\vec{E}_1(\vec{r},t)$ that existed in the absence of the volume. The same for the field H.

$$\vec{E}_d(\vec{r},t) = \vec{E}_2(\vec{r},t) - \vec{E}_1(\vec{r},t) \quad (1)$$

$$\vec{H}_d(\vec{r},t) = \vec{H}_2(\vec{r},t) - \vec{H}_1(\vec{r},t) \quad (2)$$

From Maxwell's equations, we deduce the following relationships:

$$\overrightarrow{rot}\vec{E}_d = \vec{K}_e - \mu_1 \frac{\partial \vec{H}_d}{\partial t} \quad (3)$$

$$\overrightarrow{rot}\vec{H}_d = \vec{J}_e + \sigma_1 \vec{E}_d + \varepsilon_1 \frac{\partial \vec{E}_d}{\partial t} \quad (4)$$

In these relationships $\vec{J}_e$ and $\vec{K}_e$ are vectors given by the expressions:

$$\vec{J}_e = (\sigma_2 - \sigma_1)\vec{E}_2 + (\varepsilon_2 - \varepsilon_1)\frac{\partial \vec{E}_2}{\partial t} \quad (5)$$

$$\vec{K}_e = -(\mu_2 - \mu_1)\frac{\partial \vec{H}_2}{\partial t} \quad (6)$$

The diffracted electromagnetic fields $\vec{E}_d$ and $\vec{H}_d$ comport as if they were created by the equivalent sources $\vec{J}_e$ and $\vec{K}_e$.
The relation (5) shows the role of the presence of the volume (V). indeed, the equation (6) clarifies that the volume (V) can be replaced by an equivalent source of current having the value given by the expression (5), so as to obtain the same fields $\vec{E}_d$ and $\vec{H}_d$ that can be produced by the presence of the volume (V).
We have shown that there is certain piece of information about the object relating between the object's current distribution and the diffracted field in the surrounding milieu [11]. This relation of the diffracted field $\vec{E}_d$ is written in this form.

$$\vec{E}_d(\vec{r}) = j\omega\mu_0 \int_V \overline{G}(\vec{r},\vec{r'})\vec{J}_e(\vec{r'})\,dV \quad (7)$$

$\overline{G}(\vec{r},\vec{r'})$ is the dyad related to the function of scalar Green.

3. Spectrum of the diffracted field

3.1. Definition

Having introduced the relation of the spectral representation of Green's function [11] in the expression of dyad $\overline{G}$, we found:

$$\overline{G} = \frac{j}{8\pi^2}\iint_{-\infty}^{+\infty}\frac{1}{\gamma}\begin{vmatrix} 1-\frac{\alpha^2}{K^2} & \frac{-\alpha\beta}{K^2} & \frac{-\alpha\gamma}{K^2} \\ \frac{-\alpha\beta}{K^2} & 1-\frac{\beta^2}{K^2} & \frac{-\beta\gamma}{K^2} \\ \frac{-\alpha\gamma}{K^2} & \frac{-\beta\gamma}{K^2} & 1-\frac{\gamma^2}{K^2} \end{vmatrix} \cdot \ldots e^{-j[\alpha(x-x')+\beta(y-y')+\gamma(z-z')]}d\alpha d\beta \quad (8)$$

α, β, γ : The spatial frequencies related to each direction of the wave propagation
Let's pose:

$$[\bar{g}] = -\begin{vmatrix} 1-\frac{\alpha^2}{K^2} & \frac{-\alpha\beta}{K^2} & \frac{-\alpha\gamma}{K^2} \\ \frac{-\alpha\beta}{K^2} & 1-\frac{\beta^2}{K^2} & \frac{-\beta\gamma}{K^2} \\ \frac{-\alpha\gamma}{K^2} & \frac{-\beta\gamma}{K^2} & 1-\frac{\gamma^2}{K^2} \end{vmatrix} \quad (9)$$

By introducing dyad's expression in the relation (7), we have:

$$\vec{E}_d(\vec{r}) = j\omega\mu_0 \iiint_V \left(\frac{-j}{8\pi^2}\right) \iint_{-\infty}^{+\infty} \frac{1}{\gamma} e^{-j[u,R]} d\alpha d\beta \vec{J_e}(\vec{r'}) dv \quad (10)$$

Since the integration variables were independent; we can inverse the order of integrations, posing:

$$\vec{Y}(\alpha,\beta,\gamma) = \frac{1}{\gamma} \iiint_V [\bar{g}] \vec{J_e}(\vec{r'}) e^{j[\alpha x' + \beta y' + \gamma z']} dx' d\ y' dz'$$

We obtain

$$\vec{E}_d(\vec{r}) = \frac{\omega\mu_0}{8\pi^2} \iint_{-\infty}^{+\infty} \vec{Y}(\alpha,\beta,\gamma)\ e^{-j[\alpha x+\beta y+\gamma z]} d\alpha d\beta \quad (11)$$

The useful information, the distribution of the equivalent current $\vec{J}_e(x',y',z')$ in the object's volume is, then, contained in the spectrum of the plane wave $\vec{Y}(\alpha,\beta,\gamma)$. We can therefore obtain this spectrum from the tangential components of the diffracted field $\vec{E}_d$ at each point of an equation plane (z = z0); these components are defined by the following relations demonstrated in [11], the component according to x is of the form:

$$\vec{E}_{d_x}(x,y,z_0) = \frac{\omega\mu_0}{8\pi^2} \iint_{-\infty}^{+\infty} \vec{Y}_x(\alpha,\beta,\gamma)\ e^{-j[\gamma z_0]} e^{-j[\alpha x+\beta y]} d\alpha d\beta \quad (12)$$

The component according to y is also of the same form, and the third component $\vec{E}_{d_z}(x,y,z_0)$ can be determined only if the two first ones get obtained by measure (there is no free charge in the measure plane (z = z0); then, we can write $(\mathrm{div}\vec{E}_d = 0)$.

$\vec{E}_d$ FOURIER inverse transformation is, by definition, written:

$$\vec{\varepsilon}_d(\alpha,\beta,z_0) = \frac{1}{4\pi^2} \iint_{-\infty}^{+\infty} \vec{E}_d(x,y,z_0)\, e^{j[\alpha x+\beta y]} dxdy \quad (13)$$

And automatically we have

$$\vec{E}_d(x,y,z_0) = \iint_{-\infty}^{+\infty} \vec{\varepsilon}_d(\alpha,\beta,z_0)\, e^{-j[\alpha x+\beta y]}\, d\alpha d\beta \quad (14)$$

Knowing that:

$$\vec{E}_d(x,y,z_0) = \frac{\omega\mu_0}{8\pi^2} \iint_{-\infty}^{+\infty} \vec{Y}\ (\alpha,\beta,\gamma)\ e^{-j[\gamma z_0]} e^{-j[\alpha x+\beta y]} d\alpha d\beta \quad (15)$$

We deduce:

$$\vec{\varepsilon}_d(\alpha,\beta,z_0) = \frac{\omega\mu_0}{8\pi^2} \vec{Y}(\alpha,\beta,\gamma) e^{-j[\gamma z_0]} \quad (16)$$

Either

$$\vec{Y}(\alpha,\beta,\gamma) = \frac{8\pi^2}{\omega\mu_0} e^{j[\gamma z_0]} \vec{\varepsilon}_d(\alpha,\beta,z_0) \quad (17)$$

Since the distribution of the equivalent current $\vec{J}(r')$ is zero outside the volume (v), the limits of the integral can be extended to infinity (-∞, + ∞) without changing its value.

Using the inverse transformation of Fourier $\vec{J}(x',y',z')$, the relation (10) can be written in this way:

$$\vec{Y}(\alpha,\beta,\gamma) = \frac{[\bar{g}(\alpha,\beta,\gamma)]}{\gamma} 8\pi^3 \vec{J}(\alpha,\beta,\gamma) \quad (18)$$

3.2. Conditions for the existence of the spectrum of the diffracted field

The spectrum of the diffracted field is given by the relation (17).

If we place in the case of ε1>>σ1/ω (medium with very little conductor and frequency greater than gigahertz). We will have $k^2 \neq \omega^2\mu\varepsilon 1$ from $k^2 = \alpha^2 + \beta^2 + \gamma^2$, that is to say k^2 is real.

The relation $k^2 = \alpha^2 + \beta^2 + \gamma^2$ is then of two degrees of freedom since only two parameters can be freely chosen. If α and β are independent, γ is automatically linked to them by the expression:

$$\gamma = \sqrt{k^2 - \alpha^2 - \beta^2}$$

The existence of the spectrum of the diffracted field depends on the values of γ through the term exp(j γz0).[10]

If α2 + β2 >k2 , then γ is pure imaginary and we will have: exp(-| γ|z0).--> 0 if | γ|z0 >>1. In this case, $\vec{Y}$ tends to zero; the spectrum is variable and can not be measured in the output plane.

If α2 + β2 <= k2 , then γ can be real. this condition ensures the existence of the $\vec{Y}(\alpha,\beta,\gamma)$:$(\vec{Y}(\alpha,\beta,\gamma) \# 0)$

Since the parameters α and β are spatial frequencies corresponding to real directions, we deduce that the spectrum that can be measured in the output plane corresponds only to the values of α and β for which we have:

$$\alpha^2 + \beta^2 \leq k^2 = \mu_0\varepsilon_1\omega^2$$

From this inequality, we deduce the maximum spatial frequencies accessible to the measurement: $\alpha_{max} = \omega\sqrt{\mu_0\varepsilon_1} = \frac{2\pi}{\lambda_0}\sqrt{\frac{\varepsilon_1}{\varepsilon_0}} = K_0\sqrt{\frac{\varepsilon_1}{\varepsilon_0}}$

$$\beta_{max} = \omega\sqrt{\mu_0\varepsilon_1} = \frac{2\pi}{\lambda_0}\sqrt{\frac{\varepsilon_1}{\varepsilon_0}} = K_0\sqrt{\frac{\varepsilon_1}{\varepsilon_0}}$$

with $K_0 = \frac{2\pi}{\lambda_0}$, ($\lambda_0$ the wavelength)

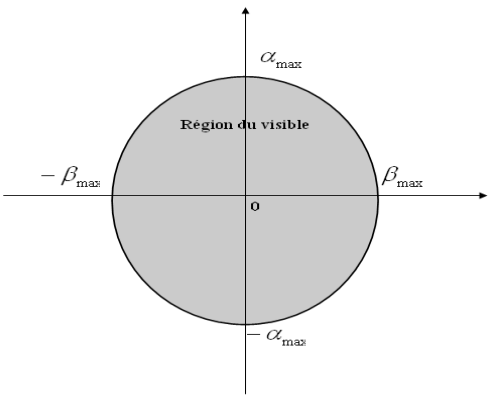

Figure 3: Spectrum existence domain

Thus, the largest spatial frequency accessible to the measurement is proportional to the square root of the relative dielectric constant of the medium in which the object is immersed. To receive the maximum information on the object, the medium in which it is located must have a very high dielectric permittivity.

In summary, the accessible spectrum $\vec{Y}(\alpha,\beta,\gamma)$ is the "visible part" of the spectrum of the function $\vec{E}_d(x,y,z_0)$ delimited by the indicated region (Fig. 3).

The existence of the spectrum $\vec{Y}(\alpha,\beta,\gamma)$, guaranteed by the preceding conditions, makes it possible to write the system of vector equations to determine the current distribution $\vec{J}(x',y',z')$:

$$\vec{Y}(\alpha,\beta,\gamma) = \frac{[\bar{g}(\alpha,\beta,\gamma)]}{\gamma} 8\pi^3 \vec{J}(\alpha,\beta,\gamma) \qquad (19)$$

with : $\gamma = \sqrt{k^2 - \alpha^2 - \beta^2}$

The reconstitution of this system requires a prior study of the nature of the $\bar{g}(\alpha,\beta)$ matrix, this is the objective of the following paragraph.

4. Inverse problem

The matrix $\left[\bar{g}(\alpha,\beta)\right]$ is defined by the equation (9) :

The calculation shows that we have : $\det[\bar{g}] = 0$

Since the determining of the equations system $\left|\vec{Y} = \bar{g}\vec{J}\right|$ is zero leads to an indetermination in the system resolution.

So the problem here is a problem of finding the values of distributing the equivalent current of an object subjected to an electromagnetic wave from the spectrum of the diffracted field measured on a plane. This problem belongs to the class of inverse problems posed in the sense of Hadamard [14][22].

In other words, the system being dealt with has many solutions. This mathematic indetermination translates exactly the ambiguity of the physical phenomena encountered in the problems of the "inverse source" and the "inverse diffraction," which means that there is an infinite number of current densities that can create the same field, or there is an infinite number of objects that can produce the same diffracted field.

One could nevertheless find the approximate solution of a degenerate system, by applying the algebraic regularization methods of Tikhonov [14][22].

The proposal of neglecting $\mathrm{div}\vec{J}(r)$ in the object leads to the hypothesis of uniformity of the current distribution in the object. This shows that the matrix $[\bar{g}]$ becomes the unified matrix $[\bar{g}] = [\bar{I}]$ [11].

5. Simulation and results

5.1. Reconstruction steps

5.1.1. Creation of the object

The first step in reconstruction is to create an object of different form. We have chosen the main forms from which any object can be made, for example: a point object; object with a linear dimension; two-dimensional object square, circular, cylindrical, hollow, several parts ... In our numerical simulation, the object will be decomposed into a number of points crossed by an equivalent current distribution which is considered constant in the object and which is zero out of the object. The data related to the simulated objects are stored in memory in the form of matrices of N*N points, they are used during the computations of the diffracted field and the precision of reconstitution of images.

$$\vec{J}(x,y,z_0) = \begin{cases} 1\ mA/m^2 & pour\ x_1 \le x \le x_2\ \ et\ \ y_1 \le y \le y_2 \\ 0 & ailleurs \end{cases}$$

5.1.2. Principal reconstruction steps

In the context of the simplification hypothesis, we can identify the main steps to be used to determine the distribution current $\vec{J}(x',y',z')$:

a) Calculated the diffracted field $\vec{E}_d(x,y,z_0)$ by an object in amplitude and phase in a plane behind the obstacle.

b) Calculated the inverse Fourier transform of this field:

$$\vec{\varepsilon}_d(\alpha,\beta,z_0) = \frac{1}{4\pi^2}\int_{-\infty}^{+\infty}\int \vec{E}_d(x,y,z_0)\ e^{j[\alpha x+\beta y]}dxdy$$

c) Calculated the plane wave spectrum $\vec{Y}(\alpha,\beta,z_0)$ in the visible region:

$$\vec{Y}(\alpha,\beta,\gamma) = \frac{8\pi^2}{\omega\mu_0} e^{j[\gamma z_0]}\vec{\varepsilon}_d(\alpha,\beta,z_0)$$

d) Calculated J, this measurable spectrum being related to the distribution current by the relation:

$$\vec{Y}(\alpha,\beta,\gamma) = \frac{-8\pi^3}{\gamma}\vec{J}(\alpha,\beta,z_0)$$

e) Calculated the distribution current $\vec{J}(x',y',z')$:

$$\vec{J}(x',y',z') = \int_{-\infty}^{+\infty}\int \vec{J}(\alpha,\beta,z_0)\ e^{-j[\alpha x+\beta y+\gamma z']}d\alpha d\beta$$

With z'= cte.

In Table. 1, the main program of the object reconstruction process witch is summarized as follows:

Table 1: Matlab Main Program

Program	Comment
clc	
clear all	
[J1,x,y,N]=objrectan(30,35,30,35,64);	% Create the object
surf(J1)	% Visualization of the original objet
[E,M,Ph,z0]=champ_diff(J1,x,y,N,2);	% Calculate the diffracted field
[S1,R1]=TFDI_2D(E);	% Calculate the spectrum of the field diffracted by the inverse Fourier transform
r1=real(S1);	
I1=imag(S1);	
M1=sqrt(r1.^2+I1.^2);	
r2=real(R1);	
I2=imag(R1);	
M2=sqrt(r2.^2+I2.^2);	
figure	
surf(M1)	% Visualization of the diffracted field spectrum
title('spectre décentré ')	

```
figure
surf(M2)
title('spectre centré ')
[Y1,A,B,G]=courant_inter(R1,N,z0);     % Calculate of the
                                        intermediate current spectrum
figure
 surf(G)
figure
surf(abs(Y1))          % Visualization of the intermediate current
                       spectrum
Je=TFD_2D(Y1);         % Calculate the equivalent distribution
figure
surf(abs(Je))          % Visualization of the reconstituted object
```

This program contains five functions (objrectan, diff_field, TFDI_2D, int_interact and TFD_2D), these functions allow to:

objrectan: Create the object

diff_field: Calculate the diffracted field

TFDI_2D: Calculates the spectrum of the field diffracted by the inverse Fourier transform of field

Courant_inter: Calculation of the intermediate current spectrum

5.2. Results of simulation

To accurately verifying the good march of the algorithm of reconstituting the distribution of an equivalent current, we have decided to make simulation tests under MATLAB in which the diffracted field is calculated instead of being measured. The application of this simulation deals with objects of different and known forms.

TV satellite transmissions use the 12GHz frequency, and, knowing that the oven microwave generates frequencies close to 2.45GHz, the fifth harmonic of the oven f5 =12,25GHz can disrupt TV satellite transmission. For this reason, we have chosen f =f5 in our simulation case.

The data of simulation are the frequency of the incidence f=12,25GHz, the distance of the observation plane z0=2*λ, digitizing pace p=λ/2, and the number of the measurement point N = 64.

By varying the shape of the object being simulated, we get the following results for simple square object (Fig. 4), object of linear dimension, punctual object, four squares object, hollow object [15].

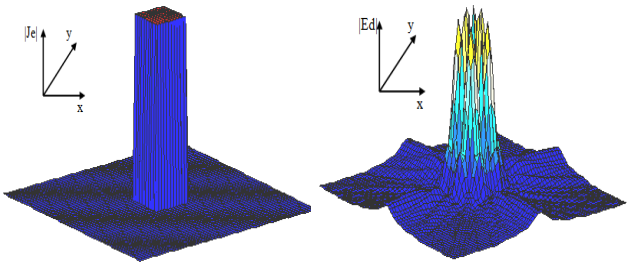

4-a: Original square object Je(x',y')

4-b: Diffracted field Ed(x, y, z0) for the square object

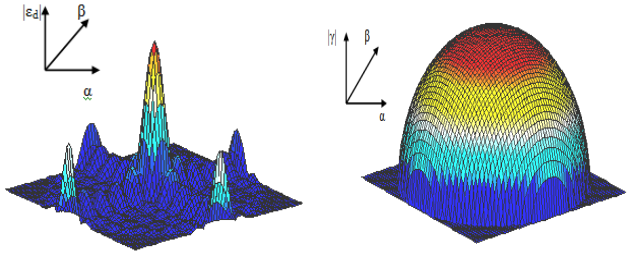

4-c: Inverse Fourier transform of the diffracted field Ed(α, β, z0)

4-d: Calculated of the γ defined the visible domain

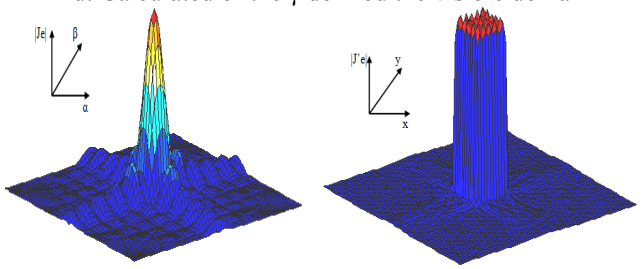

4-e: Calculated of the intermediary current Je(α, β) defined in visible domain

4-f: Calculated of the equivalent current distribution Je(x', y', z0) reconstituted object

Figure 4: Simulation results of a square object

5.3. Study of parameter influence on the reconstruction quality

Having studied the different forms of an object, The figure 5 present the result of simulation of another type of object (four squares object). What comes later focuses basically on the three main step of reconstruction.

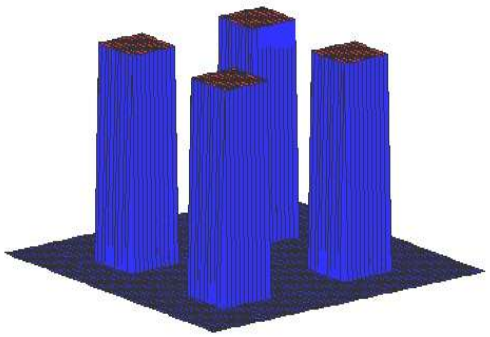

(a) Original object

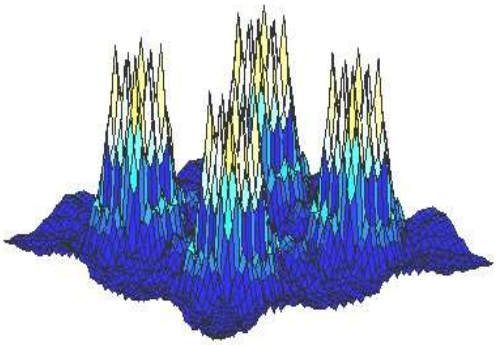

(b) Diffracted field

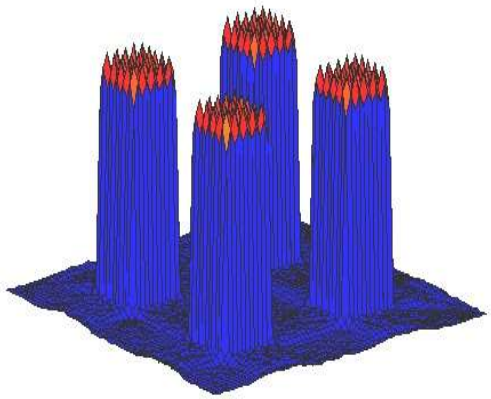

(c) Object Reconstruction

Figure 5. Simulation results of a four squares object (a) Original object; (b) Diffracted field (c) Object Reconstruction

Indeed, in view of the different objects reconstructed by our method, we find that:

- In general, the object reconstituted is clearly similar to the original object.
- The deformation at the border of the object reconstructed is more visible than elsewhere

Comparatively speaking, and as shown in Fig. 6 the object reconstruction by NK and GC methods necessitate the use of 10 iterations to have an object reconstruction; that is, to have a near object of the origin, these methods have increased the number of iteration to 150 [14,15]. They lack the important memory of execution and need to increase the time of simulation. Then again our method leads to more significant results and quickly permits to getting information about the object form.

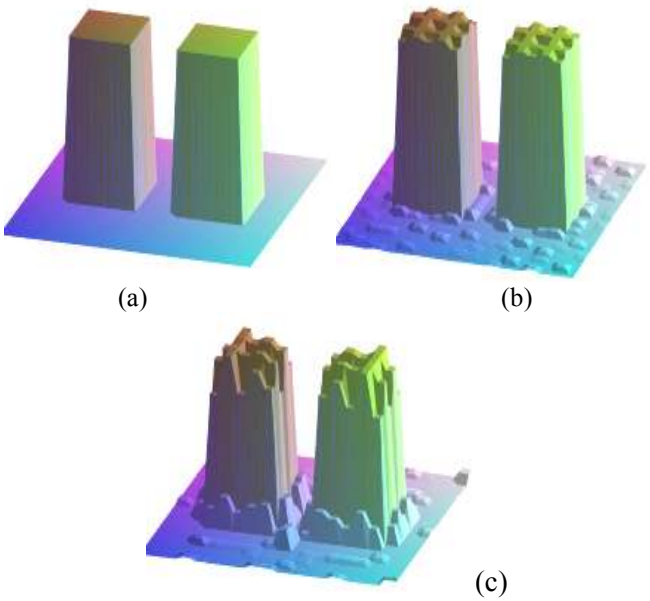

(a) (b)

(c)

Figure 6. Simulation results of a 2 squares object [14,15] (a) Object Reconstruction by Newton-Kantorovitch method (NK) after 10 iteration; (b) Object Reconstruction by Conjugate Gradiant method (GC) after 10 iteration

The method presented in this paper is based on microwaves imaging. It allows calculating the diffracted field by an object on a plane of measurement. In general, the object reconstituted is substantially similar to the original object. The deformation at the border of the object reconstructed is more visible than elsewhere.

We have studied the influence of different parameters (N number of the measurement point, and the distance z0 of the measurement plane) on the quality of reconstitution. We are going to be interested in one single type of object, such as an object of four squares, for discussing results.

5.3.1. Variation of the distance z0 of the measurement plane N=64

After expressing the relation (9) of the diffracted field, we can say that the more the distance of measurement z0 gets bigger the more the amplitude of the field becomes weak. So, if the measurement plane is sufficiently far from the source, the distance between a point of measurement and a point of source $|\vec{R}| = |\vec{r} - \vec{r'}|$ can be approximated by $|\vec{r}|$. The value of the field does not depend on coordinates of the source $|\vec{r'}|$ and therefore the field in this case loses the information and the reconstitution of the source degraded to augmenting the distance z0, as shown in Fig.7.

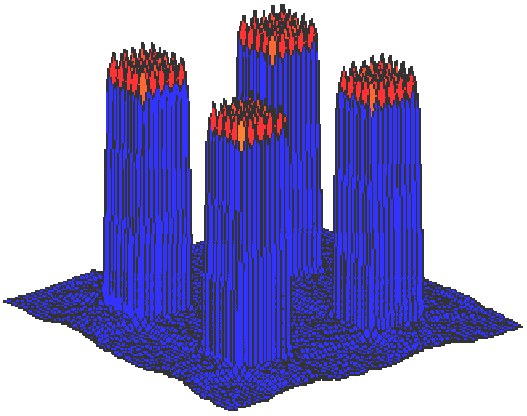

7-a): reconstituted object for N=64 et z0=4*λ.

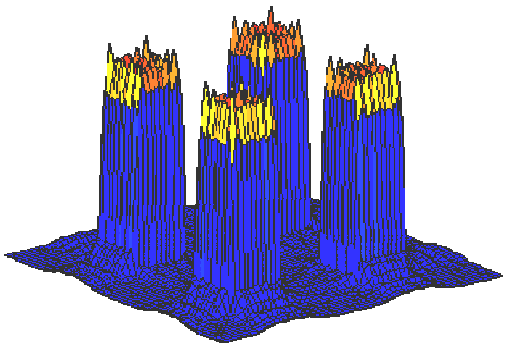

7-b): reconstituted object for N=64 et z0=7*λ.

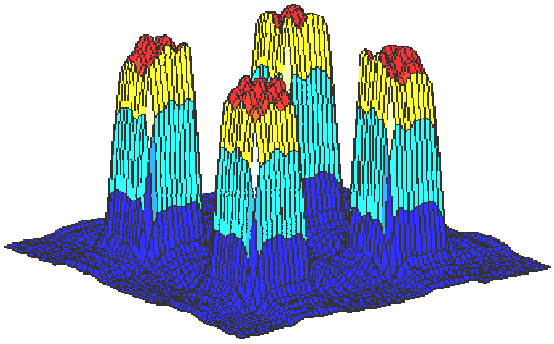

7-c): reconstituted object for N=64 et z0=15*λ.

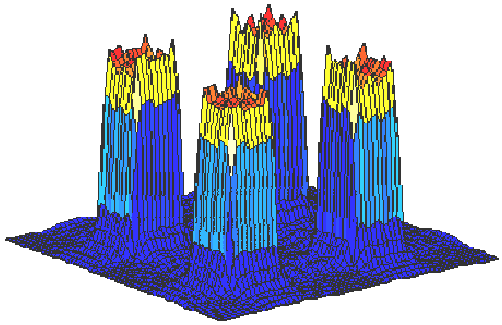

7-d): reconstituted object for N=64 et z0=25*λ.

Figure 7: Reconstituted for different distances z0.

The simulation shows that the reconstructed object is of good quality when the distance of measurement is shorter (inferior to 5*λ).

5.3.2. Variation of the measurement points N

In the microwave imaging case, theoretically speaking, the field should be measured in an infinite plane, though the measurement plane is always limited. This corresponds to a spatial truncation of field signal; in other words, the signal representing the measured field is in a finite support, hence, the oscillations in the reconstituted images are inevitable [8].

To improve this situation, we try to take the largest possible surface so that the values of the field at the edge of the measurement surface are approximately equal to zero by augmenting the number of measurement points as much as possible. But we are always to take into consideration that the augmentation of the measurement points number makes the measurement surface of the diffracted field grow, which in turn augments the time of calculation. Therefore, the choice of N number of measurement points depends on the power of the computer used.

We have made the reconstitution of images by changing the number of measurement point setting the pace of discretization (λ = no/2), we found the results shown in Fig. 8.

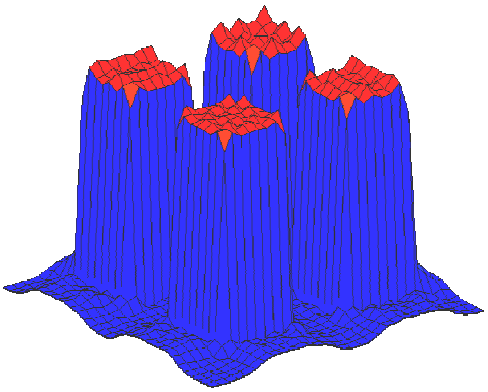

8-a): reconstituted object for N=32.

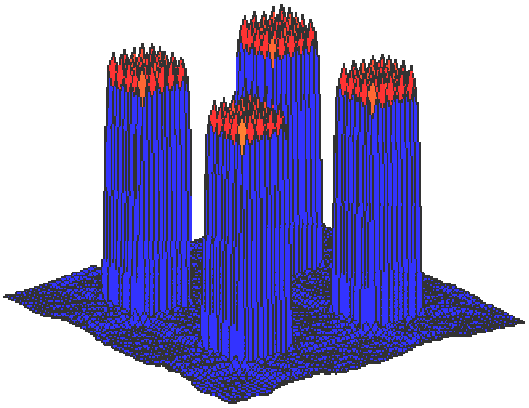

8-b): reconstituted object for N=64.

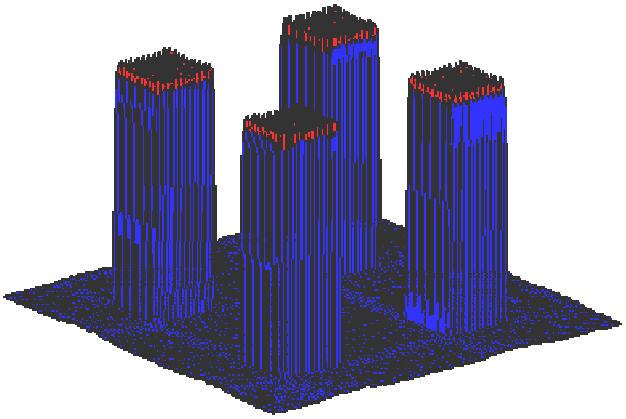

8-c): reconstituted object for N=128.

Figure 8: Reconstituted object for different numbers N of measurement point.

To deal with the problem of inverse diffraction, we pose the indetermination of our system's resolution. The proposition of neglecting $\mathrm{div}\,\vec{\psi}(\vec{r})$ [8], therefore, permits this resolution, but with errors on the border. However, we can estimate that the a priori error, theoretically committed, is acceptable. This is well justified by the results which our numerical simulation provides.

6. Conclusions

The results obtained using this method show that the choice of the number of measuring points and also the distance between the measurement plane and the source (object) affect the quality of the reconstitution. In addition, the spectral method leads to more significant results; it nevertheless allows very quickly obtaining information on the object shape.

This method permits locating sources of radiation of an ISM applicator, such as the 5th harmonic of the microwave oven. The location thereby introduces the measured values of the field radiated in the environment of the applicator in the reconstitution algorithm.

The perspectives are realization of the microwave imaging system for the detection of the objects studied, and Extension to other microwave imaging techniques for detecting and locating 3D objects.

References

[1] M. Pastorino, S. Caorsi, and A. Massa, A global optimization technique for microwave nondestructive evaluation, *IEEE Transactions on Instrumentation and Measurement* 51(4): 666–673, 2002.

[2] P. M. Meaney, M. W. Fanning, T. Raynolds, C. J. Fox, Q. Fang, C. A. Kogel, S. P. Poplack, and K. D. Paulsen, Initial clinical experience with microwave breast imaging in women with normal mammography, *Academic Radiology* 14(2): 207–218, 2007.

[3] L. P. Song, C. Yu, Q. H. Liu, Through-wall imaging (TWI) by radar: 2-D tomographic results and analyses, *IEEE Transactions on Geoscience and Remote Sensing* 43(12): 2793–2798, 2005.

[4] A. Sabouni, S. Noghanian, S. Pistorius, Experimental results for microwave tomography imaging based on fdtd and ga, *Progress In Electromagnetics Research M* 33: 69–82, 2013.

[5] Y. Mejdoub, A.GHAMMAZ, H. ROUIJAA, Reconstitution des courants de fuite des applicateurs ISM par imagerie micro-onde, *International conference, Telecom2009 and 6ème JFMMA*, Agadir, Morroco. March 11-13, 2009

[6] A. Ghammaz, S. Leffeuvre, N. Teissandier, Spectrale behavior of domestic microwave ovens and its effects on the ISM band, *annales des telecommunications* 8: 1178–1188, 2003.

[7] A. Lahham, A. Sharabati, Radiofrequency radiation leakage from microwave ovens, *Advance Radiation Protection Dosimetry,* 157(4): 488 – 490, 2013.

[8] A.J. Devaney, A computer simulation study of diffraction tomography, *IEEE Trans. Biomed. Eng* 7: 377–386, 1983.

[9] W. Tabbara, B. Duchêne, C. Pichot, D. Lesselier, L. Chommeloux, N. Joachimowicz, Diffraction tomography: contribution to the analysis of some applications in microwaves and ultrasonics. *Inverse Problems* 4: 305–331, 1988.

[10] M. F. Adams, A. P. Anderson, Three dimensional image-construction technique and its application to coherent microwave diagnostics, *Proc IEEE* 127: 138-142, 1980.

[11] C. Dourthe, *Tomographie micro-onde d'objets enterrés, Application à l'auscultation radar*. Thèse de doctorat en Géotechnique, Ecole Nationale des Ponts et Chaussées, 1997.

[12] N. Joachimowicz, C. Pichot, J.P. Hugonin, Inverse scattering: an iterative numerical method for electromagnetic imaging, *IEEE Trans. Antennas Propagat* AP-39: 1742-1752, 1991.

[13] P. Lobel, R. Kleinman, C. Pichot, L. Blanc-Féraud, M. Barlaud, Conjugate-gradient method for solving inverse scattering with experimental data, *IEEE Antennas Propag. Mag* 38: 48-51, 1996.

[14] A. Lobel, *Problèmes de diffraction inverse : reconstruction d'images et optimisation avec régularisation par préservation des discontinuités - Application à l'imagerie micro-onde*, Thèse de doctorat en Sciences de l'ingénieur, Université de Nice-Sophia Antipolis, September 1996.

[15] Y. Mejdoub, A. Ghammaz, H. Rouijaa, Electromagnetic Imaging Reconstruction from the Spectrum of the Diffracted Field, *International Journal of Microwave And Optical* Technology, 14(1): 23-30, 2019.

[16] S. Caorosi, G. L. Gragnani, M. Pastorino, Two-Dimensional Microwave Imaging by a Numerical Inverse Scattering Solution, *IEEE Trans. Microwave Theory Tech* 38: 981–989, 1990.

[17] A. Franchois, C. Pichot, Microwave imaging–complex permittivity reconstruction with a levenberg-marquardt method, *IEEE Trans. Antennas Propagat* 45: 203-215, 1997.

[18] J. De Zaeytijd, A. Franchois, C. Eyraud, J.M. Geffrin, Full-wave three dimensional microwave imaging with a regularized Gauss-Newton method, Verona, Italy - 2007.

[19] K. D. Paulsen, P. M. Meaney, M. J. Moskowitz, J.M. Sullivan, A Dual Mesh Scheme for Finite Element Based Reconstruction Algorithms, *IEEE Trans. Medical Imag* 14: 504–514, 1995.

[20] Amer Zakaria, Joe LoVetri, Application of Multiplicative Regularization to the Finite-Element Contrast Source Inversion Method, IEEE *transactions on antennas and propagation*, 59(9): 3495-3498, 2011.

[21] P. M. Meaney, Q. Fang, S. D. Geimer, A. V. Streltsov, K. D. Paulsen, 3D Scalar Microwave Image Reconstruction Algorithm, *IEEE MTT-S International Microwave Symposium Digest ,* pp. 2269–2272, 2002.

[22] M. Chouiti, *Détection et Reconstruction de forme d'Objets par les Techniques d'Imagerie Micro-ondes*, Thèse de doctorat en Sciences de l'ingénieur, Faculte des sciences, Université de Abou-bekr belkaid - Tlemcen, avril 2017.